Acta Biomaterialia 7 (2011) 2787–2796

Contents lists available at ScienceDirect

Acta Biomaterialia

journal homepage: www.elsevier.com/locate/actabiomat

A PEGylated fibrin-based wound dressing with antimicrobial and angiogenic activity

Shanmuganathan Seetharaman [a,c,1], Shanmugasundaram Natesan [a,c,1], Ryan S. Stowers [b], Conor Mullens [d], David G. Baer [a], Laura J. Suggs [b], Robert J. Christy [a,*]

[a] United States Army Institute of Surgical Research, Fort Sam Houston, TX 78234, USA
[b] Biomedical Engineering Department, University of Texas, Austin, TX 78712, USA
[c] Pittsburgh Tissue Engineering Initiative, Pittsburgh, PA 15219, USA
[d] Department of Chemistry, University of Texas, San Antonio, TX 78249, USA

ARTICLE INFO

Article history:
Received 30 December 2010
Received in revised form 8 March 2011
Accepted 7 April 2011
Available online 13 April 2011

Keywords:
Silver sulfadiazine
Chitosan
PEGylated fibrin gel
Angiogenesis
Adipose-derived stem cells

ABSTRACT

Wounds sustained under battlefield conditions are considered to be contaminated and their initial treatment should focus on decreasing this contamination and thus reducing the possibility of infection. The early and aggressive administration of antimicrobial treatment starting with intervention on the battlefield has resulted in improved patient outcomes and is considered the standard of care. Chitosan microspheres (CSM) loaded with silver sulfadiazine (SSD) were developed via a novel water-in-oil emulsion technique to address this problem. The SSD-loaded spheres were porous with needle-like structures (attributed to SSD) that were evenly distributed over the spheres. The average particle size of the SSD–CSM was 125–180 μm with 76.50 ± 2.8% drug entrapment. As a potential new wound dressing with angiogenic activity SSD–CSM particles were impregnated in polyethylene glycol (PEGylated) fibrin gels. In vitro drug release studies showed that a burst release of 27.02% in 6 h was achieved, with controlled release for 72 h, with an equilibrium concentration of 27.7% (70 μg). SSD–CSM–PEGylated fibrin gels were able to exhibit microbicidal activity at 125 and 100 μg ml^{-1} against *Staphylococcus aureus* and *Pseudomonas aeruginosa*, respectively. The in vitro vasculogenic activity of this composite dressing was shown by seeding adipose-derived stem cells (ASC) in SSD–CSM–PEGylated fibrin gels. The ASC spontaneously formed microvascular tube-like structures without the addition of any exogenous factors. This provides a method for the extended release of an antimicrobial drug in a matrix that may provide an excellent cellular environment for revascularization of infected wounds.

Published by Elsevier Ltd. on behalf of Acta Materialia Inc.

1. Introduction

Historically and as a result of improvised explosive devices being used against our military personnel in the current conflicts in Iraq and Afghanistan burn wounds comprise approximately 5–10% of all combat injuries. One of the most frequent complications in burn victims is infection, which requires immediate treatment to reduce the possibility of further complications, yet it remains one of the leading causes of mortality among burn patients [1–3]. The most prevalent infections of military burn patients are caused by the pathogenic microbes *Pseudomonas aeruginosa* and *Staphylococcus aureus*. Infections caused by these bacteria cause exudation at the wound site [4], which affects the healing process by reducing the oxygen tension, degrading extracellular matrix proteins and various growth factors, delaying re-epithelialization, and preventing wound closure [5]. Various agents have been developed in an attempt to control bacterial infection in these patients [6], but none appear to promote revascularization.

Silver sulfadiazine (SSD) is a broad spectrum antimicrobial agent that controls yeasts, molds, other types of fungi, and bacteria, including *P. aeruginosa* and *S. aureus*, as well as methicillin-resistant *S. aureus* (MRSA). SSD readily ionizes to release silver ions, which intercalate into the microbial DNA. Sulfadiazine interferes with many cellular metabolic processes, including DNA synthesis, folic acid pathways, and the respiratory electron transport system, and can interact with thiol groups on microbial proteins [7]. A standard 1% cream formulation contains silver complexed to a lipid-soluble polypropylene glycol base along with the sulfadiazine molecule [8]. Topical cream therapy requires frequent application (usually two to four changes per day) and often leads to delayed wound healing, increased trauma, and further dehiscence of the wound [9]. The hydrophobicity of the cream base tends to form an adhesive pseudo-eschar which is difficult to distinguish from a burn eschar and inhibits the penetration of SSD into burn wounds [10]. In large burns a significant number of silver ions can also be absorbed into the systemic circulation and cause toxicity [11–13]. In addition,

* Corresponding author. Tel.: +1 210 916 9528; fax: +1 210 916 3877.
E-mail address: robert.christy@us.army.mil (R.J. Christy).
[1] These authors contributed equally to this work.

1742-7061/$ - see front matter Published by Elsevier Ltd. on behalf of Acta Materialia Inc.
doi:10.1016/j.actbio.2011.04.003

Report Documentation Page

Form Approved
OMB No. 0704-0188

1. REPORT DATE	2. REPORT TYPE	3. DATES COVERED
01 JUL 2011	**N/A**	**-**

4. TITLE AND SUBTITLE	5a. CONTRACT NUMBER
A PEGylated fibrin-based wound dressing with antimicrobial and angiogenic activity	5b. GRANT NUMBER
	5c. PROGRAM ELEMENT NUMBER
6. AUTHOR(S)	5d. PROJECT NUMBER
Seetharaman S., Natesan S., Stowers R. S., Mullens C., Baer D. G., Suggs L. J., Christy R. J.,	5e. TASK NUMBER
	5f. WORK UNIT NUMBER
7. PERFORMING ORGANIZATION NAME(S) AND ADDRESS(ES)	8. PERFORMING ORGANIZATION REPORT NUMBER
United States Army Institute of Surgical Research, JBSA Fort Sam Houston, TX	
9. SPONSORING/MONITORING AGENCY NAME(S) AND ADDRESS(ES)	10. SPONSOR/MONITOR'S ACRONYM(S)
	11. SPONSOR/MONITOR'S REPORT NUMBER(S)

12. DISTRIBUTION/AVAILABILITY STATEMENT
Approved for public release, distribution unlimited

13. SUPPLEMENTARY NOTES

14. ABSTRACT

15. SUBJECT TERMS

16. SECURITY CLASSIFICATION OF:			17. LIMITATION OF ABSTRACT	18. NUMBER OF PAGES	19a. NAME OF RESPONSIBLE PERSON
a. REPORT	b. ABSTRACT	c. THIS PAGE			
unclassified	**unclassified**	**unclassified**	**UU**	**10**	

optimal application amounts of SSD cream for burn wounds have not been standardized. With this in mind, alternative antimicrobial SSD products have been developed, including water-soluble gels [14] and biomaterial-based dressings [15]. Unfortunately, these systems still lack the ability to control the release of SSD so that the silver concentration does not exceed toxic levels to patients when used for topical wound application [16].

Natural polymers are preferred over synthetic polymers in developing controlled release formulations because they mimic their in vivo counterparts. Natural polymers are also preferred because they are abundant and naturally available, cost-effective, biocompatible, and biodegradable. Among these natural polymers chitosan (poly (β-(1,4)-2-amino-2-deoxy-D-glucopyranose), a natural cationic glycosaminoglycan, has been used for wound healing applications because of its excellent biocompatibility and mucoadhesive characteristics. Reports show that chitosan, when fabricated into gels, sponges, or microcarriers, exhibits pH-sensitive swelling and drug release by diffusion through its porous structure. Microcarriers and nanocarriers made up of chitosan are widely used for controlled delivery of a wide range of therapeutics [17]. These carriers can be developed by various techniques, such as emulsion cross-linking, coacervation/precipitation, spray drying, ionic gelation, and sieving. Among these, ionic gelation is preferred for drugs that require an initial short burst release while maintaining delivery in a controlled fashion. This strategy is preferred for materials intended for wound healing applications. Apart from that, chitosan has the natural ability to interact with host cells and is also similar to the integral components of the extracellular matrix (ECM). Chitosan molecules can form ionic interactions with anionic molecules, and have been previously used for the controlled release of drugs [18]. Since SSD is a weak anionic drug it is logical to use chitosan to develop a controlled release formulation. Moreover, we have previously shown that antibiotics and stem cells can be delivered in a controlled fashion in both in vitro and in vivo systems [19–21].

Beyond drug release, it is desirable to use active polymers that can act as a platform to induce functional recruitment of host cells for wound healing. Studies show that hydrogel-based polymers can improve healing by initiating early cellular and molecular events during wound healing [22]. More importantly, infiltration of mesenchymal stem cells to the wound site is currently thought to be a crucial early event in the tissue regeneration process [23]. We have recently shown that a polyethylene glycol-based fibrin gel (PEGylated fibrin gel) induces vasculogenesis both in vitro and in vivo [24]. To exploit the inherent ability of fibrin as a substitute for a three-dimensional provisional matrix and as a carrier to control the release of SSD we designed a fibrin-based wound dressing. This dressing is expected to primarily control infection and may further aid in neovascularization when applied to an infected wound.

In this study we entrapped SSD in CSM to produce controlled and sustained release of SSD. The SSD-loaded CSM (SSD–CSM) was then impregnated into a PEGylated fibrin gel (SSD–CSM–PEGylated fibrin gel) and used as an antibacterial wound dressing. The SSD–CSM micospheres and SSD–CSM–PEGylated fibrin gel were analyzed for their in vitro release and antibacterial efficiency. Furthermore, we provide evidence that the SSD–CSM–PEGylated fibrin gel supports vascular-like tube formation by adipose-derived stem cells (ASC) in vitro.

2. Materials and methods

2.1. Preparation of CSM and SSD–CSM

CSM were prepared by a novel water-in-oil emulsification process with simultaneous ionic coacervation using our previous protocol [19]. Briefly, a water-in-oil emulsion of chitosan (Sigma–Aldrich) was prepared by slowly adding a known volume of 3% (w/v) chitosan (in 0.5 M acetic acid) to a mixed oil phase containing soya oil (Sigma–Aldrich) and *n*-octanol (Acros Organics) with span 80 (Sigma–Aldrich) as an emulsifier. The mixture was emulsified with a magnetic and an overhead stirrer simultaneously. Ionic gelation was initiated by 1% (w/v) potassium hydroxide in *n*-octanol. After cross-linking, the oil phase of the mixture containing CSM was slowly decanted and the spheres were recovered using acetone or isopropyl alcohol, sonicated (Vibracell, Viewsonics, 600 Hz) for 15 min at a constant amplitude of 42% with an intermittent on/off pulse of 9/4 s, and dried in a vacuum desiccator. For the preparation of drug-loaded microspheres, SSD (Sigma–Aldrich) at different weight percent concentrations (10 and 20 wt.%) with respect to chitosan was added in the aqueous phase and sonicated before the emulsification process.

2.2. Determination of particle size distribution

The size ranges of CSM and the SSD–CSM particles were analyzed with a laser diffraction particle size analyzer (Malvern STP2000 Spraytec). The particles were analyzed at a focal length of 328 mm using isopropyl alcohol as a non-dissolving and non-reacting dispersant. The samples were stirred constantly until completion of the analysis in order to maintain a homogeneous dispersion of the spheres.

2.3. Determination of drug content

The percentage of SSD entrapped in CSM and the amount of SSD released from the SSD–CSM particles and SSD–CSM–PEGylated fibrin gel during in vitro release studies were determined by estimating the silver release using a graphite furnace atomic absorption spectrometer (GFAAS) (Perkin–Elmer 4100ZL). For silver estimation the glass apparatus was washed with 1.5 M nitric acid for 48 h and then rinsed three or four times with deionized water and oven dried. Before silver estimation samples were digested with 5 ml of concentrated nitric acid and evaporated to dryness in a fume hood using a temperature controlled water bath. The digestion was repeated three times and the residue obtained after drying was dissolved in 1.5 ml of 0.2 N nitric acid. To estimate the silver concentration we used 20 μl injections of each sample and analyzed them in triplicate. The GFAAS was calibrated against a traceable silver standard solution utilizing a five point linear calibration in accordance with the guidelines of the National Institute of Standards and Technology. Calibration was accepted if the correlation coefficient R exceeded 0.99. The amount of SSD present in each sample was calculated using the concentration of silver and represented as means ± SD.

2.4. Morphological analysis of SSD–CSM and SSD–CSM–PEGylated fibrin gel

2.4.1. Scanning electron microscopy (SEM)

The morphological features of CSM and the SSD–CSM were assessed by SEM. For analysis the specimens were sputter-coated with gold–palladium (40–60%). The ultrastructural features of CSM and the SSD–CSM were analyzed with a JEOL JSM 5610 series scanning electron microscope equipped with an electron optical system with a 0.5–30 keV capacity electron gun and an electron detector.

2.4.2. Transmission electron microscopy (TEM)

To analyze the fine structures of SSD–CSM images were captured with a JOEL 1230 transmission electron microscope. The samples were fixed in 1 vol.% glutaraldehyde in phosphate-buf-

fered saline, rinsed twice in 0.1 M phosphate buffer for 3 min each and then placed in 1% Zetterquist's osmium for 30 min. Subsequently dehydration was performed using a series of ethanol washes (70% for 10 min, 95% for 10 min, and 100% for 20 min) and the samples were then treated twice with hexamethyldisilizane (for 5 min each). The samples were then air dried in a desiccator, washed, and infiltrated with epoxy resin. Ultrathin sections (~70 nm) were cut and mounted on copper grids.

2.5. Energy dispersive X-ray (EDAX) microanalysis

EDAX microanalysis was performed to identify silver (Ag^+) within SSD–CSM particles. The samples were sputter-coated with gold–palladium (40–60%), followed by the addition of a thin film of carbon, with a coating thickness of ~10–20 nm, to reduce charging and to improve image quality.

2.6. Preparation of SSD–CSM–PEGylated fibrin gels

PEGylated fibrinogen was prepared as previously described [24]. Briefly, succinimidylglutarate polyethylene glycol (SG-PEG-SG, 3400 Da, NOF America Corp.) was added to fibrinogen (Sigma–Aldrich) in a 6-well plate at molar ratio of 10:1 (SG-PEG-SG:fibrinogen) in Tris-buffered saline, pH 7.8, and incubated for 20 min at 37 °C. An equal volume of thrombin (Sigma–Aldrich) in 40 mM calcium chloride (final concentration 12.5 U ml^{-1}) was then added and incubated for 10 min at room temperature. The resulting gels were then rinsed twice with Hank's balanced salt solution (HBSS), pH 7.8, to remove unbound SG-PEG-SG. To prepare SSD–CSM–PEGylated fibrin, SSD–CSM particles (25 mg) were added to the SG-PEG-SG:fibrinogen mixture followed by gelation with thrombin. Fig. 1 is a schematic representation of the preparation process.

2.7. Rheologic evaluation of SSD–CSM–PEGylated fibrin gels

A rheometer (AR-G2, TA Instruments Ltd.) with parallel plate geometry was used to determine the small strain oscillatory shear behavior of SSD–CSM–PEGylated fibrin. Samples were prepared as described previously in 35 mm diameter molds with a total volume of 4 ml. The analysis was carried out at different time points (0, 24, 48, and 72 h) for samples incubated at 37 °C. For analysis the gels were placed on the bottom plate of the rheometer and the top plate was lowered until the gel contacted the entire surface. Frequency and strain sweeps were performed to determine the linear viscoelastic region of the gels. After a short pre-shear period the storage modulus (G') was measured at a constant frequency (15 rad s^{-1}) and percentage strain (1%).

2.8. Preparation of SSD–CSM–(ASC)–PEGylated fibrin gels

Human ASC from subcutaneous adipose tissue were obtained from ZenBio Inc. The SSD–CSM-(ASC)-PEGylated fibrin gels were prepared in a 6-well plate by adding passage two ASC (50,000 cells per gel) with various concentrations of SSD–CSM (2.5, 5, or 10 mg) to the SG-PEG-SG:fibrinogen solution. Gels were formed as described above (Fig. 1). The prepared SSD–CSM–(ASC)–PEGylated fibrin gels were washed twice with HBSS and incubated with alpha minimal essential medium (α-MEM) supplemented with 10% fetal bovine serum, antibiotic–antimycotic (100 U ml^{-1} penicillin G, 100 μg ml^{-1} streptomycin sulfate, and 0.25 μg ml^{-1} amphotericin B) and 2 mM L-glutamine (Invitrogen) in a 5% carbon dioxide (CO_2) humidified incubator at 37 °C. Gels were incubated for 15 days, and light micrographs were taken.

2.9. Immunocytochemical analysis of ASC in SSD–CSM–(ASC)–PEGylated fibrin gels

Day 15 gels were prepared for cryosectioning using a gradient sucrose cryopreservation technique [25]. Briefly, gels were washed with HBSS (2 × 5 min), fixed with 4% paraformaldehyde (PFA), treated serially with increasing concentrations of sucrose (5–20%) and then incubated overnight in 20% sucrose at 4 °C. The sucrose-treated gels were then embedded in a 20% sucrose–Histoprep (Fisher) mixture (2:1) and flash frozen. Sections, 10–12 μm thick, were cut with a cryostat (Leica Microsystems), washed with sterile HBSS and fixed with 4% PFA for 20 min. Non-specific Fc receptor-mediated sites were blocked by incubating the sections for 1 h with 5% goat serum in HBSS and washed with HBSS (2 × 5 min). The sections were then incubated with

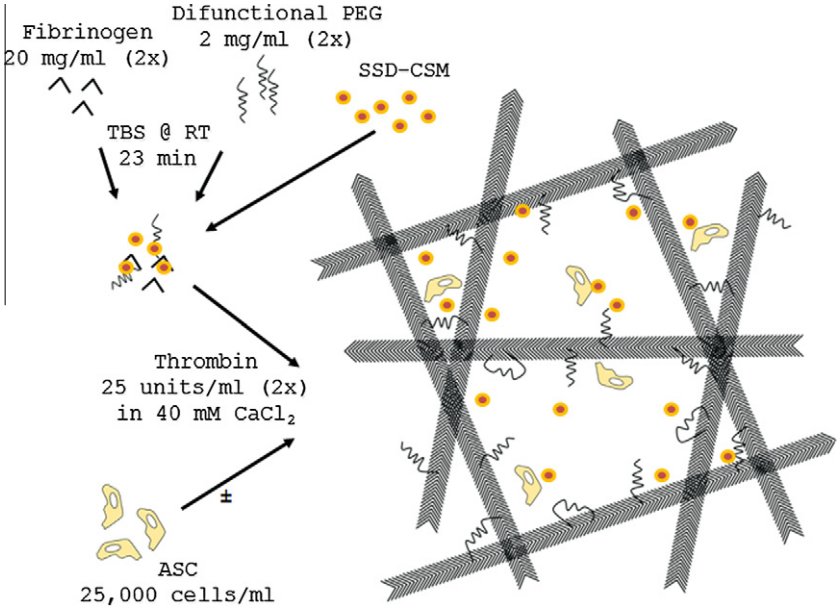

Fig. 1. Schematic diagram representing the preparation of SSD-loaded CSM in a PEGylated fibrin gel.

human-specific monoclonal antibodies to chrondroitin sulfate proteoglycan (NG2) (10 μg ml^{-1}, Millipore) or platelet-derived growth factor receptor β (PDGFRβ) antibodies (10 μg ml^{-1}, BD Biosciences). Following incubation with primary antibodies the sections were then washed with HBSS (2 × 5 min) and incubated with 5 μg ml^{-1} host species-specific Alexa Fluor 594 secondary antibodies (Invitrogen) for 45 min at 4 °C. Finally, the sections were washed twice (5 min) and nuclei stained with Hoechst 33342 (Invitrogen). Non-specific fluorescence was assessed using sections incubated with the respective fluorophore-labeled secondary antibodies.

2.10. In vitro release studies

In vitro release kinetics of SSD from SSD–CSM and SSD–CSM–PEGylated fibrin gels was determined using a Franz diffusion model finite dosage apparatus (PermeGear) [26]. To determine the release of silver from SSD–CSM particles we spread 25 mg of microspheres uniformly over a semipermeable membrane of type I rat tail collagen isolated by our previously described protocol [27]. To determine the release of silver from SSD–CSM–PEGylated fibrin we directly cast a gel as described above containing 25 mg SSD–CSM in the donor compartment of the Franz apparatus. The Franz apparatus receptor compartment contained synthetic serum electrolytic solution (SSES) composed of 0.601 g sodium chloride, 0.235 g sodium bicarbonate, 0.0283 g disodium hydrogen phosphate, and 0.0284 g sodium sulfate per 100 ml at 37 °C with constant stirring. Aliquots of the samples were withdrawn at 6, 12, 24, 48, and 72 h from the receptor compartment and analyzed for the amount of SSD released by determining silver concentration using a GFAAS. The experiments were carried out in triplicate and the amount of drug released was expressed as a percentage with respect to time. The release of SSD was also determined under complete sink conditions (release determined by immersing the SSD–CSM and SSD–CSM–PEGylated fibrin in SSES) under similar experimental conditions.

2.11. Antibacterial efficiency determination

Antibacterial activity of the SSD–CSM and SSD–CSM–PEGylated fibrin gels was determined for *P. aeruginosa* (ATCC 25619) and *S. aureus* (ATCC 9144) using the tube dilution method [28,29]. Initial inocula of these strains were prepared by setting up five colonies from a fresh overnight culture plate in trypticase soy broth (Teknova) for *S. aureus* or Mueller–Hinton broth (Teknova) for *P. aeruginosa*. The liquid cultures were incubated at 37 °C to optical density of 0.1 (≡0.5 McFarland) at a wavelength of 600 nm. From this culture 100 μl was transferred to 10 ml of fresh Mueller–Hinton broth and incubated to the logarithmic growth phase, 0.5 McFarland (10^8 c.f.u. ml^{-1}). The cultures were appropriately diluted to produce $5 \times 10^5 - 1 \times 10^6$ c.f.u. ml^{-1} and used as primary inocula. Different amounts of SSD–CSM (7.5–15 mg) were introduced into the flasks with the primary inocula and incubated at 37 °C for 72 h. Samples were withdrawn at different time intervals (24, 48, and 72 h) to determine the minimal inhibitory concentration (MIC) and minimal bactericidal concentration (MBC) and mean number of survivors at MBC. For each experiment a control sample was subjected to a microbial count, before analysis, to determine the primary inoculum concentration. Each experiment was carried out in triplicate and is represented as the mean susceptible concentration of SSD ± SD.

2.12. Statistical analysis

One-way ANOVA was performed in this study to determine the significant difference in the release rates between SSD–CSM and SSD–CSM–PEGylated fibrin gel. $P < 0.001$ was considered statistically significant.

3. Results

3.1. SSD-loaded chitosan microspheres

Chitosan was selected as the carrier material to deliver SSD because it is a unique polycationic polymer with excellent biocompatibility and biodegradable characteristics. To date SSD has been the drug of choice for burn wound infection. The sonication of SSD with chitosan resulted in a homogeneous colloidal mixture. This mixture, when subjected to a water-in-oil emulsification process with simultaneous ionic coacervation technique using KOH as a cross-linker, resulted in the formation of uniform spheres. With this procedure more than 90% of the microspheres were within the size range 125–180 μm, and <10% of the microspheres were below 100 μm (Fig. 2). SSD–CSM particles prepared at an initial drug concentration of 10 wt.% with respect to chitosan resulted in the formation of microspheres within the 125–180 μm size range and a percentage SSD entrapment of 76.50 ± 2.8%. Processes involving higher initial drug concentrations (20 wt.% SSD with respect to chitosan) resulted in the formation of some irregularly shaped particles when observed through a light microscope (data not shown). Hence, further experiments were carried out with 10 wt.% SSD as the ideal initial drug concentration.

3.2. Morphological characteristics of SSD–CSM and EDAX analysis

SEM images of CSM without SSD have a uniform size and a porous surface (Fig. 3A and B). The crevices on the surface indicate that the microspheres were formed by diffusion-controlled ionic gelation from the core. After entrapment of SSD into the microspheres (SSD–CSM) the spheres have an irregular surface with needle-like crystals of SSD (Fig. 3C and D). The SSD–CSM particles were slightly smaller than the CSM, which may be attributed to the loss or shrinkage of pores due to the ionic interaction of SSD with chitosan.

When the spheres were subjected to EDAX analysis a clear energy dispersion peak at 3.0 keV confirmed the presence of SSD in the microspheres (Fig. 3E). TEM ultrastructural analysis of SSD–CSM particles provided evidence for the presence of needle-like SSD crystals entrapped within the pores of the microspheres (Fig. 3F–H).

3.3. SSD–CSM–PEGylated fibrin gel dressing

The SSD–CSM–PEGylated fibrin gel dressing (Fig. 4A, photograph) contained uniformly dispersed SSD–CSM in the gel (Fig. 4B, photomicrograph). In our previous studies a mixture of fibrinogen with modified PEG (SG-PEG-SG) showed improved mechanical stability compared with fibrinogen alone [24]. Rheologic analysis of PEGylated fibrin gels and SSD–CSM–PEGylated fibrin gels showed that they exhibited similar mechanical stiffnesses of 82–92 Pa ($n = 3$) at 0 h (Fig. 4C), while SSD–CSM–PEGylated fibrin gels showed a mechanical stiffness of 76–86 Pa ($n = 3$) over a period of 72 h (Fig. 5C).

3.4. Release kinetics of SSD

These experiments were carried out using a Franz diffusion finite dosage apparatus, a widely accepted ex vivo release model, as well as complete sink conditions to assess the release rate kinetics of SSD–CSM alone and after impregnation into PEGylated fibrin gels. Using a Franz diffusion cell apparatus SSD followed first order

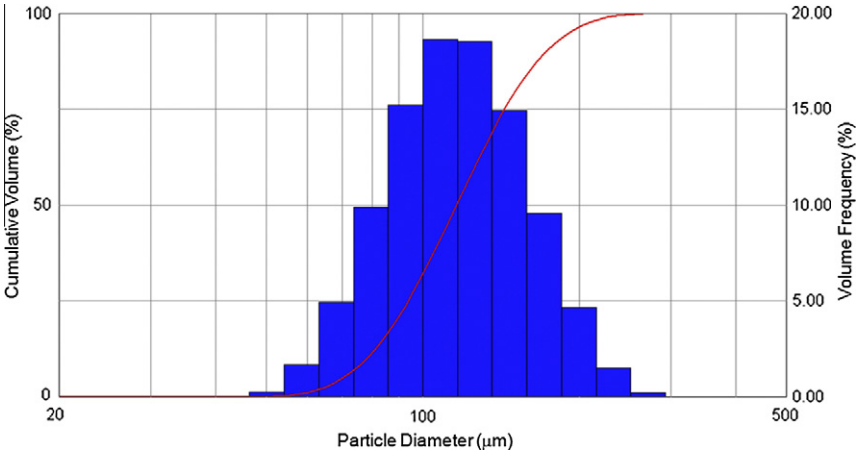

Fig. 2. Particle size distribution of SSD–CSM. The microsphere size was analyzed using a Malvern particle size analyzer. The distribution pattern indicates that more than 90% of the microspheres are between 125 and 180 μm in diameter and less than 10% of the microspheres are below 100 μm.

release kinetics. We observed that 35.48 μg ml^{-1} SSD had been released from SSD–CSM by 6 h. An equilibrium drug concentration of 37.52 μg ml^{-1} was achieved by 12 h, and was maintained at this level for 72 h. In the case of SSD–CSM–PEGylated fibrin gels there was a slight initial burst release of 73.23 μg ml^{-1}, after which the concentration decreased to 67.5 μg ml^{-1} by 12 h, an equilibrium state which was maintained for 72 h (Fig. 5A). Using complete sink conditions larger burst release concentrations were observed at 6 h for both SSD–CSM (65.1 μg ml^{-1}) and SSD–CSM–PEGylated fibrin gels (99.5 μg ml^{-1}) and steady-state release profiles were not maintained (Fig. 5B). These results show that the SSD–CSM–PEGylated fibrin gel dressing possesses ideal characteristics for a dressing intended to be applied topically to infected wounds.

3.5. Antibacterial efficiency of SSD–CSM and SSD–CSM–PEGylated fibrin gel

Microbial susceptibility concentrations for the standard pathogens *P. aeruginosa* and *S. aureus* to SSD–CSM and SSD–CSM–PEGylated fibrin gel are shown in Table 1. For both SSD–CSM and SSD–CSM–PEGylated fibrin gels the MIC against *P. aeruginosa* was observed to be 9 mg (90 ± 1.0 μg ml^{-1} SSD) and the MBC was 10 mg (100 ± 0.25 μg ml^{-1} SSD). For SSD–CSM the MIC was observed to be 12.5 mg (125 ± 0.75 μg ml^{-1} SSD) and MBC was 15 mg (150 ± 1.25 μg ml^{-1} SSD) against *S. aureus*. In the case of SSD–CSM–PEGylated fibrin gels MIC and MBC against *S. aureus* were found to be 10 mg (100 ± 1.5 μg ml^{-1} SSD) and 12.5 mg (125 ± 1 μg ml^{-1} SSD), respectively. Although an observable number of survivors (*P. aeruginosa* and *S. aureus*) were seen at 24 h, complete inhibition was achieved after 48 h. Throughout this experiment the SSD–CSM–PEGylated fibrin gel remained intact, showing no degradation in the presence of the microbes at MBC.

3.6. SSD–CSM–PEGylated fibrin gel supports tube formation by ASC

ASC demonstrate an ability to proliferate and express a characteristic phenotype within PEGylated fibrin gels analogous to our previous observation [24]. ASC demonstrated extensive tube formation in PEGylated fibrin gels at an initial cell seeding density of 50,000 cells per gel (2 ml) by day 7 (Fig. 6A). When ASC were seeded at the same cell density in SSD–CSM–PEGylated fibrin gels, containing 5 mg SSD–CSM, they exhibited formation of their characteristic tube-like structures at day 15 (Fig. 6B and C).

3.7. Immunophenotype of the tube-like structures formed in the SSD–CSM–PEGylated fibrin gel

The tube-like structures formed by ASC in the presence of SSD–CSM were found to exhibit a pericyte cell phenotype. This was confirmed through immunocytochemical staining for NG-2 and PDGFRβ (Fig. 7A and B), indicating that the prepared SSD–CSM–PEGylated fibrin gel will support stem cell in-growth and differentiation.

4. Discussion

The negative influence of infection on burn wound healing is a significant clinical challenge. The infection and/or further invasion of burn wounds populated by pathogenic microbes are mitigated by topical application of antibacterial/antimicrobial agents. Wound dressings currently used have been designed using biocompatible polymers or composites incorporating the desired antibacterial agents [30]. Chitosan-based carrier systems, ranging from microspheres to nanospheres, have been shown to be advantageous for a wide range of drug delivery applications [31]. Chitosan has been well studied as an excellent mucoadhesive polymer, but there are limited studies on the use of chitosan in the form of microcarriers for wound healing applications. In this study we show that a CSM prepared by an ionic gelation process with KOH [19] offers polycationic sites that can potentially interact with anionic molecules, either as a delivered drug or the anionic surfaces of host cells. There are processes that involve the preparation of CSM with covalent cross-linkers. Although these procedures result in the formation of uniform and stable microcarriers, the cationic nature of their surfaces is reduced because of covalent cross-links [32]. We have previously shown that ionic gelation with KOH in an oil phase effectively conserves the cationic sites of chitosan while maintaining stable cross-links [19]. Typically, lower molecular weight drugs are entrapped with reduced efficiency and require higher initial drug concentrations to achieve the required incorporation [33]. In contrast, the current study demonstrates that the polycationic sites of chitosan readily interact with Ag^+ ions present in SSD and form a weak ionic bond during drug loading. The higher percentage drug entrapment (76.50 ± 2.8 wt.%) may be attributed to the effects of a weak charge interaction.

Our previous investigations have demonstrated that microspheres more than 100 μm in diameter do not gain entry into the systemic circulation [34]. In this study over 90% of the SSD–CSM were distributed within the 125–180 μm size range (Fig. 2).

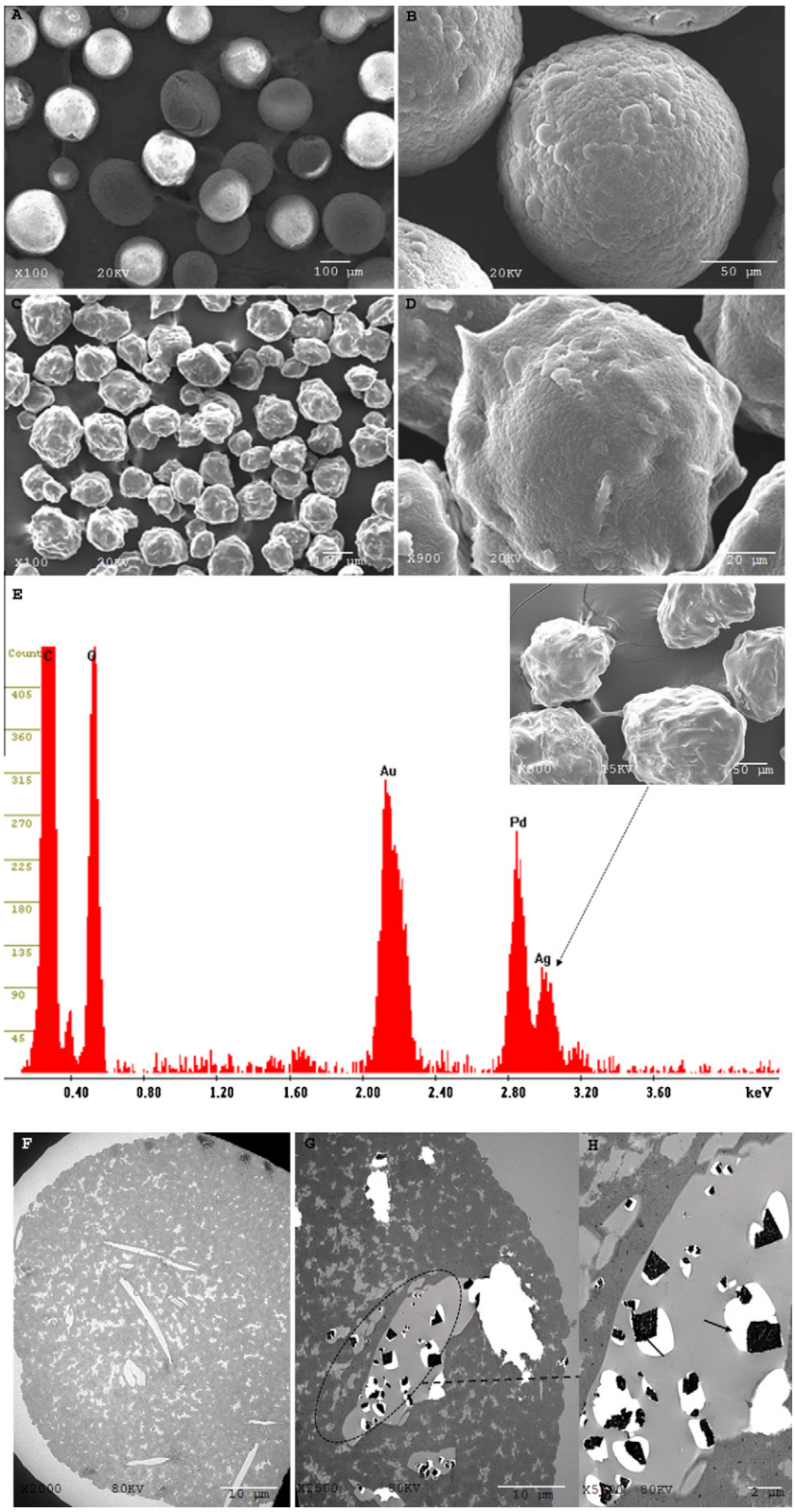

Fig. 3. Morphological features of CSM and SSD–CSM. (A) A SEM low magnification micrograph (100×) shows uniform sized microspheres. (B) A high magnification SEM micrograph (500×) shows the porous nature of the CSM. (C, D) The presence of SSD (SSD–CSM) on the exterior of microspheres gives them an irregular surface with needle-like crystals of SSD (C, 100×; D. 900×). (E) Elemental energy dispersive X-ray microanalysis of SSD–CSM confirms the presence of silver ions showing a characteristic and distinct energy dispersion peak at 3.0 keV (300×). (F–H) TEM images of SSD–CSM show the presence of needle-like SSD crystals entrapped within the CSM and distributed evenly from the core to the surface of the microsphere (F, 2000×; G, 2500×; H, 5000×).

Following drug entrapment the microspheres developed an irregular morphology because of the crystalline nature of the entrapped SSD. SEM analysis of the drug-loaded microspheres showed the presence of needle-like projections on the surface of the micro-

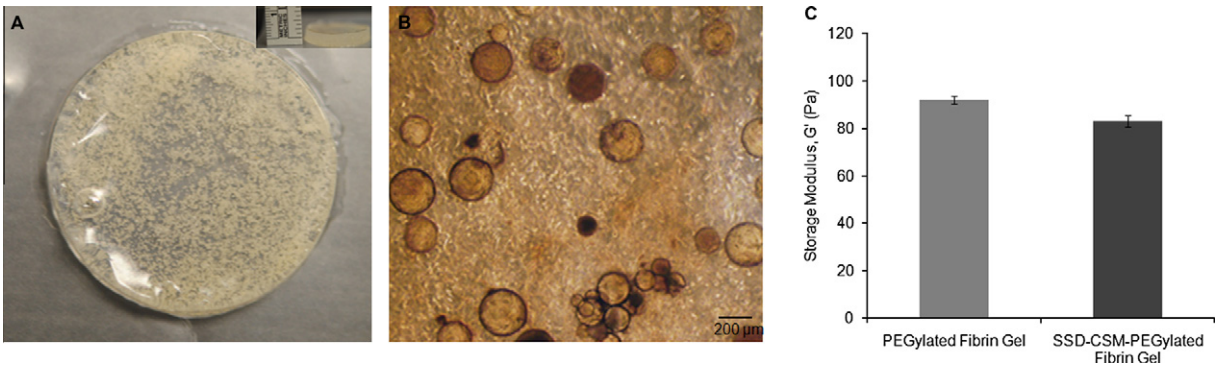

Fig. 4. (A) Photograph of a SSD–CSM–PEGylated fibrin gel. The inset shows the thickness of the gel. (B) Light microscopic image of a SSD–CSM–PEGylated fibrin gel showing the uniform dispersion of SSD–CSM. (C) Rheology data shows that the PEGylated fibrin gel and SSD–CSM–PEGylated fibrin gel exhibit similar storage moduli.

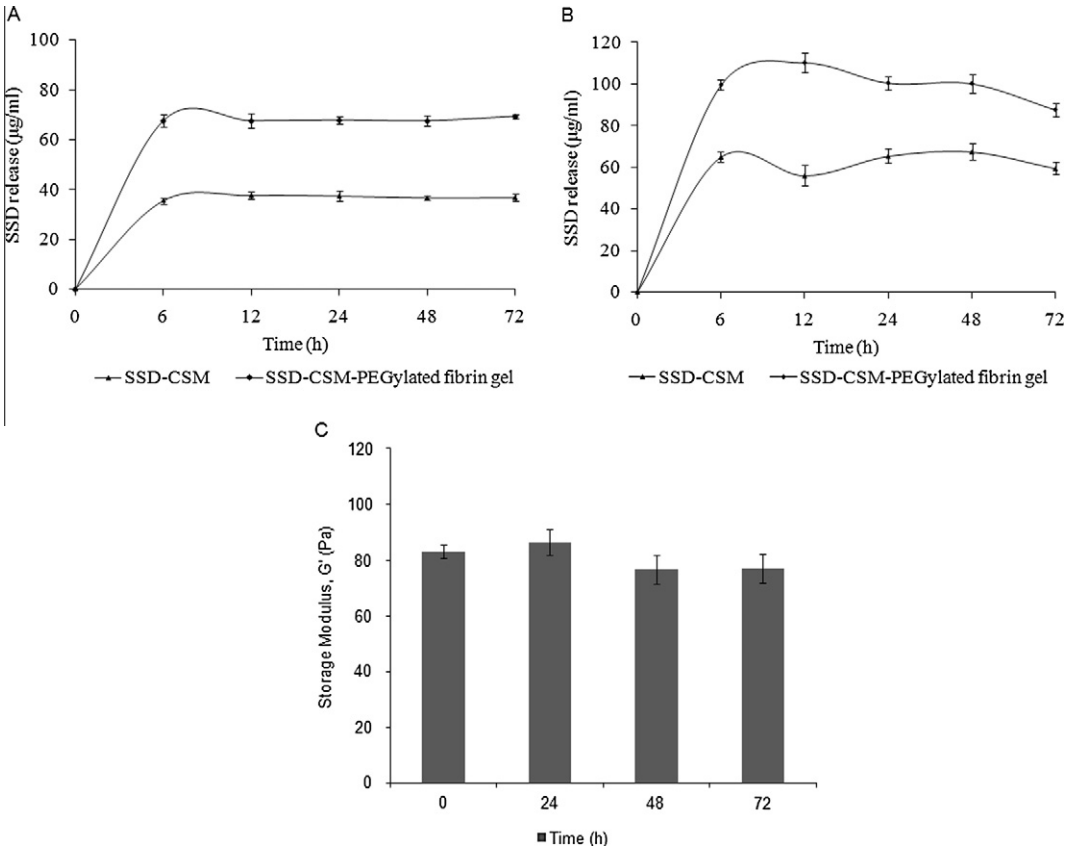

Fig. 5. In vitro controlled release profile of SSD. (A, B) SSD (μg ml^{-1}) release was measured from SSD–CSM alone and SSD–CSM in PEGylated fibrin gels (±SD) over a 72 h period (A) using a Franz apparatus or (B) under sink conditions. (C) Rheology data indicate that the SSD–CSM–PEGylated fibrin gel maintained mechanical stability for up to 72 h. One-way ANOVA, $P < 0.001$, between SSD–CSM and SSD–CSM–PEGylated fibrin gel, in both the Franz apparatus and under sink conditions, shows significant difference in the release rates at all the time points.

spheres (Fig. 3C and D). TEM analysis showed that the drug was entrapped throughout, from the surface to the core of the sphere, as was apparent by the vacant areas left after sectioning the needle-like structures within the microspheres (Fig. 3F). Presence of the drug within the microspheres was further confirmed by EDAX analysis, showing a characteristic and distinct energy dispersion peak at 3.0 keV (Fig. 3E). As a result of the EDAX analysis it was obvious that after complete processing the microspheres were devoid of any metallic ion contamination, particularly K^+ ions used during preparation of the microspheres.

To further develop an active antibacterial wound dressing we impregnated SSD–CSM into a PEGylated fibrin-based hydrogel matrix (Fig. 1). In infected wounds there is a demand for an active polymer-based wound dressing to control infection. Hydrogels in general have gained usefulness as a moist wound dressing material and have been reported to minimize pain during and between dressing changes [35]. In particular, the local application of antibacterials/antibiotics as hydrogels can provide therapeutic drug concentrations at the site of infection and can prevent systemic effects. The difunctionalized polyethylene glycol (SG-PEG-SG) has electrophilic groups at both ends that can react with protein amine groups, producing stable linkages. The SG-PEG-SG, when mixed with fibrinogen, formed PEGylated fibrin hydrogels in situ through thrombin-assisted enzymatic gelation [24]. Mechanical stability is extremely important for any hydrogel-based dressing intended for wound healing applications [24,36]. When SSD-loaded CSM were

Table 1
Minimum inhibitory concentration (MIC) and minimum bactericidal concentration (MBC) values of SSD–CSM and SSD–CSM–PEGylated fibrin gel for two standard ATCC reference strains.

Bacterial strain	SSD–CSM					SSD–CSM–PEGylated fibrin gel				
	MIC ($\mu g\ ml^{-1}$)	MBC ($\mu g\ ml^{-1}$)	Mean survivor no. after $3log_{10}$ reduction (MBC)			MIC ($\mu g\ ml^{-1}$)	MBC ($\mu g\ ml^{-1}$)	Mean survivor no. after $3log_{10}$ reduction (MBC)		
			24 h	48 h	72 h			24 h	48 h	72 h
P. aeruginosa ATCC 25619	90	100	37	<20	<20	90	100	185	25	<20
S. aureus ATCC 9144	125	150	30	<20	<20	100	125	32	<20	<20

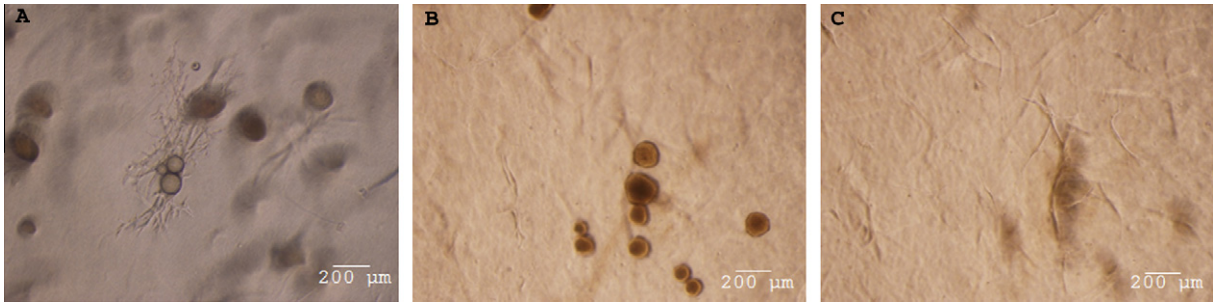

Fig. 6. Light microscopic images of ASC tube formation. (A) ASC seeded in a PEGylated fibrin gel showing tube-like structures. (B, C) ASC seeded in a SSD–CSM–PEGylated fibrin gel containing 5 mg SSD–CSM focused on the (B) CSM beads and (C) similar tube-like networks.

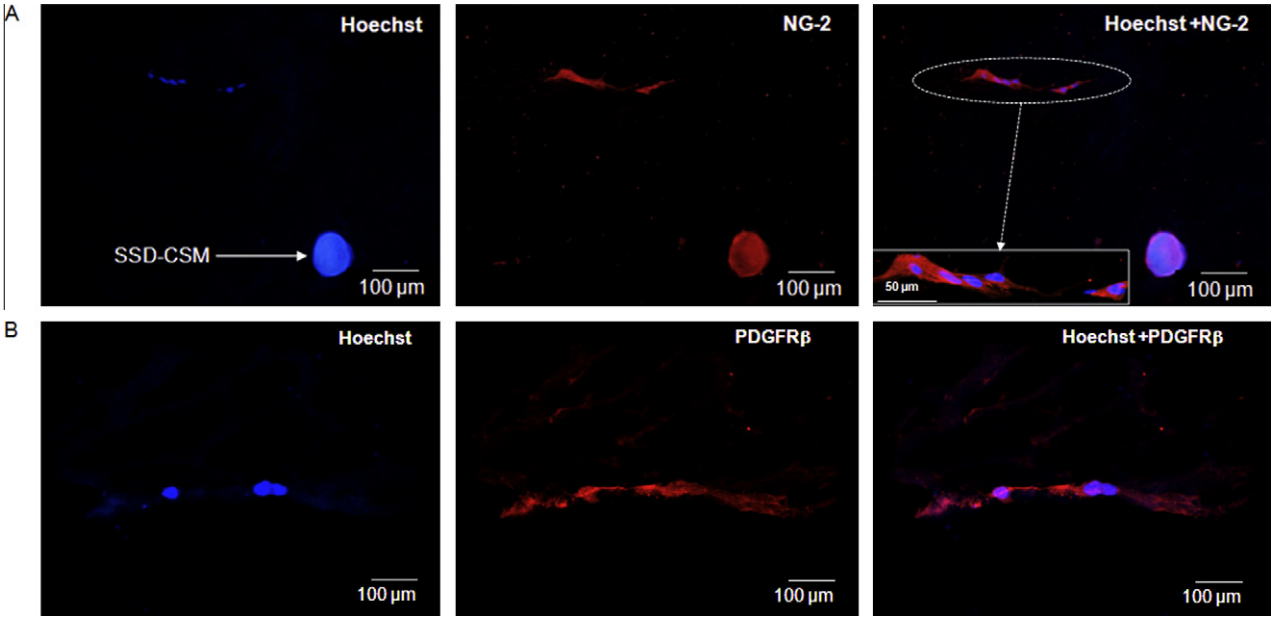

Fig. 7. Immunohistochemical staining of ASC in a SSD–CSM–PEGylated fibrin gel. The tube-like structures formed by ASC in the SSD–CSM–PEGylated fibrin gel stained with pericyte cell markers (A) NG-2 and (B) PDGFRβ and Hoechst for nuclei identification.

mixed with a functionalized PEG–fibrinogen solution mixture stable gels were formed without any loss of mechanical integrity and maintained their storage modulus over a 72 h period (Fig. 5C).

In order to analyze the phenomenon of drug release from SSD–CSM and SSD–CSM–PEGylated fibrin gels we performed SSD release kinetics experiments under simulated in vivo conditions (with SSES as the sink medium). SSD–CSM release kinetics under complete sink conditions demonstrated a large burst (65.1 µg) followed by non-steady-state release (59.4 µg) of SSD (Fig. 5B). To closely mimic the conditions of an open wound we used a Franz cell finite dosage apparatus to determine the SSD release kinetics (Fig. 5A) from CSM using collagen as a semi-permeable membrane barrier. Drug release followed first order kinetics, with an initial burst of 35.5 µg at 6 h and an equilibrium concentration of 38 µg for 72 h. The release kinetics of SSD from CSM impregnated in a PEGylated fibrin gel plug showed a similar phenomenon of first order release kinetics. In comparison with SSD–CSM alone, the SSD–CSM–PEGylated fibrin gel showed a reduced burst release of 27% and maintained controlled release for 72 h. The observed concentration (67 µg) of drug released would cover a broad spectrum of bacterial susceptibility [37]. This result indicates that the gel formulations described here would control drug release at a higher equilibrium rate (67 µg for 72 h). The increased drug release from CSM impregnated in a PEGylated fibrin gel may be due to the fact that SG-PEG-SG increases the hydrophilicity of fibrin and the ionization of Ag^{+}, leading to enhanced diffusion of the drug. The observed pattern of drug release would be suitable for wounds colonized by pathogenic microbes requiring immediate dosage

with an antibacterial agent followed by a steady-state concentration within the microbicidal range. It would also aid in stopping the progression of infection during the healing process.

The susceptibility of *S. aureus* and *P. aeruginosa* (the most prevalent pathogens of burn wounds) to SSD–CSM and SSD–CSM–PEGylated fibrin gels was determined through the tube dilution method [29]. The observed concentrations of SSD released from PEGylated fibrin gels were within the required bactericidal concentrations. The antibacterial study clearly shows that a SSD–CSM–PEGylated fibrin gel could exhibit an MBC of 12.5 mg (125 $\mu g\ ml^{-1}$ SSD), whereas SSD–CSM exhibits an MBC of 150 $\mu g\ ml^{-1}$, corroborating the drug release kinetics observed in our Franz cell diffusion experiments. It should be noted that the MBC values were calculated with respect to the amount of total drug present in the microspheres, which is expected to be released in a controlled fashion and, hence, the MBC levels are on the high side of the concentration range. The actual amount of released drug would be less and would depend on the rate of release and equilibrium concentration of SSD present at the wound site. Taking into account that a dressing is intended to remain on the wound site for at least 3 days, we designed and validated the experiment to determine the survivor count up to 72 h (Table 1).

Most wound dressings are primarily designed to address infection, with less focus on the quality of healing [38]. The SSD–CSM–PEGylated fibrin gel dressing has been designed to combat wound infection and to provide an active medium that could induce angiogenesis to hasten the healing process. It is well known that active healing progresses through the recruitment and migration of host cells in and around the wound site, as well as infiltration by host circulating cells [39]. Mesenchymal stem cells residing in the tissue may also be recruited to the wound site to initiate the reparative process. Few reports show that exogenously delivered mesenchymal stem cells from adipose tissue can hasten wound healing [40] with the aid of a provisional matrix. One of the objectives in designing a fibrin-based hydrogel dressing is to provide a viable environment for the host cells to granulate and to provide a scaffold for better wound regeneration. Recently we have shown that ASC embedded in PEGylated fibrin gels form vascular-like structures in vitro and exhibit enhanced vasculogenesis in vivo [41]. In this study we show that the impregnated SSD–CSM at a concentration of 50 $\mu g\ ml^{-1}$ allows active tube formation by ASC in vitro (Fig. 6B and C) and the morphology of the tube-like structures formed in vitro is comparable with the gels without SSD–CSM. Moreover, the tube-like structures exhibited phenotypic characteristics of pericytes (NG-2$^+$ and PDGFRβ^+, Fig. 7A and B), which are considered to be vital for further endothelial cell infiltration during neo-vascularization [42]. Therefore, it is anticipated that when applied in vivo SSD–CSM–PEGylated fibrin gels may act as an active platform inducing vasculogenesis in an infected wound environment.

5. Conclusions

The currently developed SSD–CSM–PEGylated fibrin wound dressing delivers SSD in a controlled manner within a defined bactericidal concentration for a period of 3 days. The ability of the dressing to support tubular network formation by ASC will hasten infected wound healing through induction of neovascularization.

Acknowledgements

This study was supported by funding from a DRMRP Grant (W81XWH-09-1-0607). The authors would like to thank Dr. David Zamora, Ms. Nicole L. Wrice, and Ms. Sharanda K. Hardy for isolation of adipose tissue and technical support. S. Seetharaman and S. Natesan are supported by a Postdoctoral Fellowship Grant from the Pittsburgh Tissue Engineering Initiative (PTEI). The authors thank Dr. Robert Reddick, Medical Director, and Lauren Chesnut, Technical Director of the Electron Microscopy Facility at The University of Texas Health Science Center, Department of Pathology, for use of the facility and assistance in the analysis of electron micrographs. The authors also extend their thanks to TherapeUTex Preclinical Core Lab, Drug Dynamics Institute, College of Pharmacy, University of Texas at Austin for performing the rheology studies.

The opinions or assertions contained herein are the private views of the authors and are not to be construed as official or reflecting the views of the Department of Defense or the US government. The authors are employees of the US government and prepared this work as part of their official duties. All this work was supported by the US Army Medical Research and Materiel Command.

Appendix A. Figures with essential colour discrimination

Certain figures in this article, particularly Figs. 1–4, 6 and 7 are difficult to interpret in black and white. The full colour images can be found in the on-line version, at doi:10.1016/j.actbio.2011.04.003).

References

[1] Church D, Elsayed S, Reid O, et al. Burn wound infections. Clin Microbiol Rev 2006;19:403–34.
[2] Keen EF, Robinson BJ, Hospenthal DR, Aldous WK, Wolf SE, Chung KK, et al. Incidence and bacteriology of burn infections at a military burn center. Burns 2010;36(4):461–8.
[3] D'Avignon LC, Saffle JR, Chung KK, Cancio LC. Prevention and management of infections associated with burns in the combat casualty. J Trauma 2008;64(Suppl. 3):S277–86.
[4] Kennedy P, Brammah S, Wills E. Biofilm and a new appraisal of burn wound sepsis. Burns 2010;36(1):49–56.
[5] Guo S, Dipietro LA. Factors affecting wound healing. J Dent Res 2010;89(3):219–29.
[6] Masterton RG. The new treatment paradigm and the role of carbapenems. Int J Antimicrob Agents 2009;33(2):105–10.
[7] Modak SM, Fox CL. Binding of silver sulfadiazine to the cellular components of *Pseudomonas aeruginosa*. Biochem Pharmacol 1973;22:2391–404.
[8] Stanford W, Rappole BW, Fox Jr CL. Clinical experience with silver sulfadiazine, a new topical agent for control of *Pseudomonas* infections in burns. J Trauma 1969;9:377–88.
[9] Muller MJ, Hollyoak MA, Moaveni Z, Brown TL, Herndon DN, Heggers JP. Retardation of wound healing by silver sulfadiazine is reversed by aloe vera and nystatin. Burns 2003;29(8):834–6.
[10] Harrison HN. Pharmacology of sulfadiazine silver. Its attachment to burned human and rat skin and studies of gastrointestinal absorption and extension. Arch Surg 1979;114:281–5.
[11] Tsipouras N, Rix CJ, Brady PH. Solubility of silver sulfadiazine in physiological media and relevance to treatment of thermal burns with silver sulfadiazine cream. Clin Chem 1995;41:87–91.
[12] Tsipouras N, Rix CJ, Brady PH. Passage of silver ions through membrane-mimetic materials, and its relevance to treatment of burn wounds with silver sulfadiazine cream. Clin Chem 1997;43:290–301.
[13] Sano S, Fujimori R, Takashima M, Itokawa Y. Absorption, excretion and tissue distribution of silver sulfadiazine. Burns 1982;8:278–85.
[14] Gear AJ, Hellewell TB, Wright HR, Mazzarese PM, Arnold PB, Rodeheaver GT, et al. A new silver sulfadiazine water soluble gel. Burns 1997;23:387–91.
[15] Kawai K, Suzuki S, Tabata Y, Taira T, Ikada Y, Nishimura Y. Development of an artificial dermis preparation capable of silver sulfadiazine release. J Biomed Mater Res 2001;57:346–56.
[16] Maitre S, Jaber K, Perrot JL, Guy C, Cambazard F. Increased serum and urinary levels of silver during treatment with topical silver sulfadiazine. Ann Dermatol Venereol 2002;129(2):217–9.
[17] Remunan-Lopez C, Bodmeier R. Mechanical, water uptake and permeability properties of crosslinked chitosan glutamate and alginate films. J Control Release 1997;44:215–25.
[18] Lakshmi TS, Shanmugasundaram N, Shanmuganathan S, Karthikeyan K, Meenakshi J, Babu M. Controlled release of 2,3 desulfated heparin exerts its anti-inflammatory activity by effectively inhibiting E-selectin. J Biomed Mater Res A 2010;95(1):118–28.
[19] Shanmuganathan S, Shanmugasundaram N, Adhirajan N, Ramyaa Lakshmi TS, Babu M. Preparation and characterization of chitosan microspheres for doxycycline delivery. Carbohyd Polym 2008;73:201–11.

[20] Lakshmi TS, Shanmugasundaram N, Shanmuganathan S, Babu M. Efficacy of desulfated heparin mitigating inflammation in rat burn wound model. Appl Biomater 2011;97(2):215–23.
[21] Natesan S, Baer DG, Walters TJ, Babu M, Christy RJ. Adipose-derived stem cell delivery into collagen gels using chitosan microspheres. Tissue Eng Part A 2010;16(4):1369–84.
[22] Guo X, Park H, Young S, Kretlow JD, Van den Beucken JJ, Baggett LS, et al. Repair of osteochondral defects with biodegradable hydrogel composites encapsulating marrow mesenchymal stem cells in a rabbit model. Acta Biomater 2010;6(1):39–47.
[23] Lim SM, Oh SH, Lee HH, Yuk SH, Im GI, Lee JH. Dual growth factor-releasing nanoparticle/hydrogel system for cartilage tissue engineering. J Mater Sci Mater Med 2010;21(9):2593–600.
[24] Zhang G, Wang X, Wang Z, Zhang J, Suggs L. A PEGylated fibrin patch for mesenchymal stem cell delivery. Tissue Eng 2006;12(1):9–19.
[25] Barthel LK, Raymond PA. Improved method for obtaining 3-microns cryosections for immunocytochemistry. J Histochem Cytochem 1990;38(9):1383–8.
[26] Franz TJ. The finite dose technique as a valid *in vitro* model for the study of percutaneous absorption in man. Curr Probl Dermatol 1978;7:58–68.
[27] Shanmugasundaram N, Ravikumar T, Babu M. Comparative physico-chemical and *in vitro* properties of fibrillated collagen scaffolds from different sources. J Biomater Appl 2004;18:247–64.
[28] Bowler P. The anaerobic and aerobic microbiology of wounds: a review. Wounds 1998;10:170–8.
[29] Clinical Laboratory Standards Institute. Methods for dilution antimicrobial susceptibility tests for bacteria that grow aerobically. Approved Standard. eight ed. CLSI, Wayne, Pennsylvania:2009.M07-A8.ISBN: 1-56238-689-1.
[30] Szycher M, Lee SJ. Modern wound dressings: a systematic approach to wound healing. J Biomater Appl 1992;7(2):142–213.
[31] Arya N, Chakraborty S, Dube N, Katti DS. Electrospraying: a facile technique for synthesis of chitosan-based micro/nanospheres for drug delivery applications. J Biomed Mater Res B Appl Biomater 2009;88(1):17–31.
[32] George M, Abraham TE. Polyionic hydrocolloids for the intestinal delivery of protein drugs: alginate and chitosan – a review. J Control Release 2006;114(1):1–14.
[33] Giovagnoli S, Blasi P, Ricci M, Schoubben A, Perioli L, Rossi C. Physicochemical characterization and release mechanism of a novel prednisone biodegradable microsphere formulation. J Pharm Sci 2008;97(1):303–17.
[34] Shanmugasundaram N, Sundaraseelan J, Uma S, Selvaraj D, Mary B. Design and delivery of silver sulfadiazine from alginate microspheres-impregnated collagen scaffold. J Biomed Mater Res B Appl Biomater 2006;77(2):378–88.
[35] Burd A. Evaluating the use of hydrogel sheet dressings in comprehensive burn wound care. Ostomy Wound Manage 2007;53(3):52–62.
[36] Liu H, Collins SF, Suggs LJ. Three-dimensional culture for expansion and differentiation of mouse embryonic stem cells. Biomaterials 2006;27(36):6004–14.
[37] US Pharmacopeia. Official Monographs: Silver Sulfadiazine Cream, USP 24-NF19. Rockville, MD, US, 1999. p. 1567.
[38] Baghel PS, Shukla S, Mathur RK, Randa R. A comparative study to evaluate the effect of honey dressing and silver sulfadiazene dressing on wound healing in burn patients. Indian J Plast Surg 2009;42(2):176–81.
[39] Caviggioli F, Vinci V, Salval A, Klinger M. Human adipose-derived stem cells: isolation, characterization and applications in surgery. ANZ J Surg 2009;79(11):856.
[40] Jackson WM, Nesti LJ, Tuan RS. Potential therapeutic applications of muscle-derived mesenchymal stem and progenitor cells. Expert Opin Biol Ther 2010;10(4):505–17.
[41] Zhang G, Drinnan CT, Geuss LR, Suggs LJ. Vascular differentiation of bone marrow stem cells is directed by a tunable three-dimensional matrix. Acta Biomater 2010;6(9):3395–403.
[42] Ozerdem U, Stallcup WB. Early contribution of pericytes to angiogenic sprouting and tube formation. Angiogenesis 2003;6(3):241–9.